Pastra-Landis, S. C., Evans, D. R., & Lipscomb, W. N. (1978) *J. Biol. Chem. 253*, 4624-4630.
Perutz, M. F. (1989) *Q. Rev. Biophys. 22*, 139-236.
Pflugrath, J. W., Saper, M. A., & Quiocho, F. A. (1984) in *Methods and Applications in Crystallographic Computing* (Hall, S., & Ashiaka, T., Eds.) pp 404-407, Clarendon Press, Oxford, U.K.
Phillips, J. C., Bordas, J., Foote, A. M., Koch, M. H. J., & Moody, M. F. (1982) *Biochemistry 21*, 830-834.
Porter, R. W., Modebe, M. O., & Stark, G. R. (1969) *J. Biol. Chem. 244*, 1846-1859.
Reichard, P., & Hanshoff, G. (1956) *Acta Chem. Scand. 10*, 548-566.
Sabot, M., Cini, R., Haromy, T., & Sundaralingam, M. (1985) *Biochemistry 24*, 7827-7833.
Schachman, H. K. (1988) *J. Biol. Chem. 263*, 18583-18586.
Sobottka, S. E., Cornick, G. G., Kretsinger, R. H., Rains, R. G., Stephens, W. A., & Weissman, L. J. (1984) *Nucl. Instrum. Methods 220*, 575-581.
Stevens, R. C., Gouaux, J. E., & Lipscomb, W. N. (1990) *Biochemistry* (preceding paper in this issue).
Suter, P., & Rosenbusch, J. P. (1977) *J. Biol. Chem. 252*, 8136-8141.
Swenson, D., Baenziger, N. C., & Coucouvanis, D. (1978) *J. Am. Chem. Soc. 100*, 1932-1934.
Thiry, L., & Hervé, G. (1978) *J. Mol. Biol. 125*, 515-539.
Wacks, D. B., & Schachman, H. K. (1985) *J. Biol. Chem. 260*, 11651-11658.
Wild, J. R., Loughrey-Chen, S. J., & Corder, T. S. (1989) *Proc. Natl. Acad. Sci. U.S.A. 86*, 46-50.
Wiley, D. C., & Lipscomb, W. N. (1968) *Nature (London) 218*, 1119-1121.
Xu, W., Pitts, M. A., Middleton, S. A., Kelleher, K. S., & Kantrowitz, E. R. (1988) *Biochemistry 27*, 5507-5515.
Zhang, Y., & Kantrowitz, E. R. (1989) *Biochemistry 28*, 7313-7318.
Zhang, Y., Ladjimi, M. M., & Kantrowitz, E. R. (1988) *J. Biol. Chem. 263*, 1320-1324.

Absolute Action Spectrum of E-$FADH_2$ and E-$FADH_2$-MTHF Forms of *Escherichia coli* DNA Photolyase†

Gillian Payne and Aziz Sancar*
Department of Biochemistry and Biophysics, University of North Carolina School of Medicine, Chapel Hill, North Carolina 27599-7260

Received March 9, 1990; Revised Manuscript Received May 10, 1990

ABSTRACT: *Escherichia coli* DNA photolyase mediates photorepair of pyrimidine dimers occurring in UV-damaged DNA. The enzyme contains two chromophores, 1,5-dihydroflavin adenine dinucleotide ($FADH_2$) and 5,10-methenyltetrahydrofolylpolyglutamate (MTHF). To define the roles of the two chromophores in the photochemical reaction(s) resulting in DNA repair and the effect of DNA structure on the photocatalytic step, we determined the absolute action spectra of the enzyme containing only $FADH_2$ (E-$FADH_2$) or both chromophores (E-$FADH_2$-MTHF), with double- and single-stranded substrates and with substrates of different sequences in the immediate vicinity of the thymine dimer. We found that the shape of the action spectrum of E-$FADH_2$ matches that of the absorption spectrum with a quantum yield $\phi(FADH_2) = 0.69$. The action spectrum of E-$FADH_2$-MTHF is also in a fairly good agreement with the absorption spectrum with $\phi(FADH_2\text{-MTHF}) = 0.59$. From these values and from the previously established properties of the two chromophores, we propose that MTHF transfers energy to $FADH_2$ with a quantum yield of $\phi_{\epsilon T} = 0.8$ and that $^1FADH_2$ singlet transfers an electron to or from the dimer with a quantum yield $\phi_{ET} = 0.69$. The chemical nature of the chromophores did not change after several catalytic cycles. The enzyme repaired a thymine dimer in five different sequence contexts with the same efficiency. Similarly, single- and double-stranded DNAs were repaired with the same overall quantum yield.

DNA photolyases repair cyclobutane dipyrimidine dimers occurring in UV-irradiated DNA in a light-driven reaction. Photolyases isolated from *Escherichia coli* and *Saccharomyces cerevisiae* contain two chromophores (Jorns et al., 1984; Sancar et al., 1987b), $FADH_2$[1] (Sancar & Sancar, 1984) and 5,10-methenyltetrahydrofolylpolyglutamate (MTHF) (Johnson et al., 1988). The $FADH_2$ cofactor of the *E. coli* enzyme becomes oxidized to the neutral blue radical ($FADH^0$) during purification (Payne et al., 1987). Similarly, the MTHF cofactor is gradually lost during various stages of purification. Therefore, *E. coli* photolyase preparations contain variable amounts of MTHF in addition to the catalytically inert $FADH^0$ (Payne et al., 1987). Because of these experimental artifacts, it has been difficult to assign specific roles to each chromophore and to define their mechanisms of action in the ultimate photochemical repair process.

Action spectrum measurements by Sancar et al. (1987a) with photolyase in the form in which it is purified (containing stoichiometric $FADH^0$ and 20-50% MTHF) revealed some

†This work was supported by NIH Grant GM31082.

[1] Abbreviations: $FADH_2$, 1,5-dihydroflavin adenine dinucleotide; $FADH^0$, neutral blue radical flavin adenine dinucleotide; MTHF, 5,10-methenyltetrahydrofolylpolyglutamate; T4 endo V, T4 phage endonuclease V (UV endonuclease); EDTA, ethylenediaminetetraacetic acid; DTT, dithiothreitol; ET, electron transfer; ϵT, energy transfer; ϵ, molar extinction coefficient; ϕ, quantum yield; T<>T, cyclobutane thymine dimer; bp, base pair.

0006-2960/90/0429-7715$02.50/0

unexpected features. First, the quantum yield of repair was much lower than that predicted from photolytic cross-section ($\epsilon\phi$) measurements in vivo (Harm et al., 1970). Second, the shape of the action spectrum did not match the shape of the enzyme absorption spectrum, especially in the visible region (400–700 nm) where absorption is largely due to $FADH^0$. These results led to the proposal that the catalytically active form of photolyase contains $FADH_2$ and that the apparent activity exhibited by the E-$FADH^0$ form of the enzyme was an experimental artifact. In support of this, it was found that enzyme-bound $FADH^0$ undergoes photoreduction to $FADH_2$ with a quantum yield of 0.05–0.10 (Heelis & Sancar, 1986; Heelis et al., 1987) and that the photoreduced enzyme repaired pyrimidine dimers with a quantum yield of 0.44 (Payne et al., 1987). Similarly, dithionite reduction of photolyase resulted in a severalfold increase in the photolytic cross section ($\epsilon\phi$) at 384 nm. With use of an extinction coefficient (ϵ_{384}) of 18 100 M^{-1} cm^{-1}, it was proposed that the quantum yield of the enzyme was near unity (Sancar et al., 1987a).

The identification of the second chromophore as 5,10-methenyltetrahydrofolate (Johnson et al., 1988), the realization that photolyase preparations contained substoichiometric MTHF, and the subsequent development of a method for supplementing photolyase with MTHF (Hamm-Alvarez et al., 1989) made it possible for quantum yield measurements to be conducted with enzyme of both defined chromophore composition and defined redox state. In this paper we have performed action spectrum measurements with enzyme containing $FADH_2$ only and enzyme containing a full complement of both $FADH_2$ and MTHF and demonstrated that the latter is the in vivo form of the enzyme. From these measurements we have calculated the quantum yield of repair for the two forms of enzyme, and from the quantum yields of the two forms we have been able to estimate the quantum yield of two proposed photochemical processes: energy transfer from MTHF to $FADH_2$ ($\phi_{\epsilon T}$ = 0.8) and electron transfer from $FADH_2$ to T<>T (ϕ_{ET} = 0.69). The photochemical reactions are not influenced by the primary and secondary structures of DNA, and the chromophores do not undergo any structural change at the end of the catalytic cycle. Furthermore, by using a very sensitive assay for measuring photodimer repair, we have been able to extend the action spectrum of photolyase to the far-UV. Thus, we have demonstrated that 254 nm, which is the wavelength most commonly used for making pyrimidine photodimers, is also as efficient as near-UV (300–500 nm) in photoreactivation.

Materials and Methods

Enzymes. Photolyase was purified from *E. coli* MS09 by modification of a previously described procedure (Sancar et al., 1984). Briefly, the enzyme was precipitated from cell-free extract with 55% saturated ammonium sulfate and then separated by sequential chromatography on blue Sepharose (Sigma), Bio-Gel P-100 coarse (Bio-Rad), and hydroxylapatite (Bio-Rad) resins. Photolyase purified in this manner was greater than 98% pure and contained approximately stoichiometric amounts of $FADH^0$ and substoichiometric (20–50%) MTHF. Occasionally, when oxidation to E-FAD_{ox} occurred, the enzyme was photoreduced to E-$FADH_2$ by use of trace amounts of 5-deazariboflavin, 15 mM EDTA, and irradiation at 313 nm under anaerobic conditions (Massey & Hemmerich, 1978). Exposure to oxygen results in reoxidation of E-$FADH_2$ to E-$FADH^0$.

Photolyase containing only $FADH_2$ and no MTHF was prepared by selective photodecomposition of MTHF (Heelis et al., 1987) with two Vivitar 2500 flash units set to discharge simultaneously or by irradiation at 366 nm from black light (UV-Products Blak-Ray longwave lamp) at a rate of about 700 erg mm^{-2} s^{-1} for 30 min while the enzyme was kept on ice to prevent heat denaturation. This treatment breaks MTHF into various folate degradation products which do not absorb at $\lambda > 300$ nm and no longer bind to the enzyme (Hamm-Alvarez et al., 1989). Photodecomposition was monitored spectrophotometrically by the decrease in absorption at 384 nm with a Hewlett-Packard 8451A diode array spectrophotometer. E-$FADH^0$ was readily photoreduced to E-$FADH_2$ with 100–150 filtered (long-pass 630-nm Schott RG630) camera flashes under anaerobic conditions. The cuvette was cooled on ice after 25 flashes to prevent denaturation of the enzyme. Photoreduction was monitored spectrophotometrically by the loss of longwave (450–700 nm) absorption. Photolyase containing stoichiometric amounts of both chromophores was prepared by supplementing the enzyme with MTHF as described by Hamm-Alvarez et al. (1989). Briefly, folinic acid (5-formyltetrahydrofolate) (Sigma) was converted to MTHF by incubating a 1–2 mM solution in 0.01 N HCl at 4 °C for 1–3 days. The conversion was monitored spectrophotometrically by the peak shift from 266 to 358 nm. Following conversion, MTHF at 2–10-fold molar excess was added to photolyase in storage buffer containing 50 mM Tris-HCl, pH 7.4, 100 mM NaCl, 2 mM EDTA, 20 mM dithiothreitol, and 50% glycerol and incubated on ice in the dark for 30 min. Free MTHF decays to 10-formylfolate at pH 7.4 during the incubation, but the binding to photolyase occurs sufficiently rapidly to result in stoichiometric incorporation of MTHF under these conditions. Unbound folate was removed by passing the sample through a Penefsky column (Penefsky, 1977; Hamm-Alvarez et al., 1989) equilibrated with photolyase storage buffer. E-$FADH^0$-MTHF was converted to E-$FADH_2$-MTHF without affecting MTHF by photoreduction with camera flashes filtered through 630-nm long-pass filters.

T4 endonuclease V (T4 endo V, UV endonuclease) was prepared from *E. coli* AB2480/ptac*den V* (Valerie et al., 1985) by a procedure developed by Dr. A. Ganesan (Stanford University). The cells were grown to A_{600} = 0.6 in Luria broth containing 50 μg/mL ampicillin and then induced with 1 mM isopropyl β-D-thiogalactoside for 12 h. The cells were collected and resuspended in $^1/_{20}$ culture volume of 10 mM Tris-HCl, pH 8.0, 100 mM NaCl, 10 mM EDTA, and 150 mM sucrose. The cells were lysed by incubation on ice for 30 min with 23 μg/mL lysozyme (Sigma) and 0.23% Brij-58 (Sigma). The cell debris was removed by centrifugation at 100000*g* for 60 min. The supernatant was dialyzed against 10 mM Tris-HCl, pH 8.0, 100 mM NaCl, 10 mM EDTA, and 10% ethylene glycol and stored on ice or at −80 °C until further use. The enzyme preparation contained about 10 units of T4 endo V/μL and was free of nonspecific endonucleases when tested in the presence of 1 mM EDTA.

Substrates. For the action spectrum measurements the substrate was a synthetic 48-mer duplex containing a centrally located thymine–thymine cyclobutane dimer (Husain & Sancar, 1987; Husain et al., 1988). The duplex was constructed by hybridizing and ligating six complementary oligomers of which the internal ones were radiolabeled with [γ-^{32}P]ATP by use of T4 polynucleotide kinase (Bethesda Research Lab.). Single-stranded substrate was obtained by heating the 48-mer duplex in photolyase buffer for 5 min at 95 °C followed by rapid cooling on ice. This substrate remained single stranded during quantum yield measurements as evidenced by its resistance to the restriction enzymes *Bam*HI

and *Bgl*II, which incise the duplex.

The substrates used for testing the effect of neighboring sequences on the quantum yield of repair were 20-bp duplexes containing single thymine cyclobutane dimers. Single-stranded 20-mers with T<>T and their complementary oligomers were kindly provided by Dr. J.-S. Taylor and D. Svoboda (Washington University, St. Louis, MO). Each T<>T-containing oligomer was mixed with the complementary strand and radiolabeled with [γ-^{32}P]ATP by use of T4 polynucleotide kinase. The DNA was extracted with phenol and ether and precipitated with ethanol with 1 μg of oyster glycogen (Sigma) as carrier. The two strands were annealed by resuspending approximately 20 pmol of each in 100 μL of 10 mM Tris-HCl, pH 7.4, 75 mM NaCl, and 1 mM EDTA and heating at 65 °C for 20 min, followed by slow cooling to room temperature.

Instrumentation. Quantitative photoreactivation was conducted on an integrated monochromator–actinometer (Quantacount-Photon Technology International, Inc., Princeton, NJ). The instrument houses a 75-W xenon lamp focused onto a $f/4$ grating monochrometer (1200 L/mm; 300-nm blaze) equipped with an electronically operated shutter. Monochromatic (4-nm band pass/mm slit width) light exits the monochromator and enters the sample compartment where it is split into the sample beam (~90%) and the reference beam (~10%) by the beam splitter. Behind the reference and sample cuvettes are the reference and sample detectors, each of which consists of a solution of totally absorbing rhodamine B and a large-area silicon photocell for monitoring the rhodamine B fluorescence. An electrical signal from each silicon cell is delivered to the Quantacount electronics where it is amplified and converted to a voltage signal. The electronic component continuously subtracts the sample detector signal from the reference detector signal and integrates over time. The instrument is set so that the reference signal minus the sample signal is equal to zero before sample irradiation. Because under our experimental conditions the sample beam intensity rather than the actual quanta absorbed by the sample is of primary interest, a completely absorbing screen is placed between the sample cuvette and the sample detector. Since light is prevented from reaching the sample detector, the quantum counter accumulates counts proportional to the intensity of the sample beam, integrated over the time of irradiation. The counter was calibrated with ferrioxalate actinometry (Hatchard & Parker, 1956; Calvert & Pitts, 1966) so that the counts can be converted to the total fluence to which the sample is exposed.

Photoreactivation. (*A*) *Near-UV–Visible.* Either E-FADH^0 or E-FADH^0-MTHF (12 μM) was mixed with DNA substrate (ca. 0.5–2.5 nM 48-mer or ca. 0.2 nM 20-mer) in 700 μL of photolyase buffer (50 mM Tris-HCl, pH 7.4, 50 mM NaCl, 1 mM EDTA, 20 mM DTT, 100 μg/mL BSA) containing 1.7% lactate and 20 μL of Oxyrase (Oxyrase Inc., Ashland, OH). The reaction mixture was divided into two 350-μL aliquots and placed in anaerobic cuvettes with rubber septa. The cuvettes were deoxygenated for 30 min by blowing oxygen-scrubbed (S/P disposable oxygen trap G5301-3) argon through photolyase buffer and into the cuvettes through small needles placed in the septa. Following deoxygenation, photolyase was photoreduced by filtered camera flashes. Photoreduction of FADH^0 to FADH$_2$ and maintenance of this oxidation state were monitored spectrophotometrically. Neither the photoreduction treatment nor spectrophotometric measurements in the course of the assay resulted in any appreciable repair of substrate (see Results). Following photoreduction a 25-μL sample was removed from the cuvette with a gas-tight syringe that had been rinsed in a deoxygenated solution of dithionite, followed by rinsing in deoxygenated deionized H_2O. The cuvette was then placed in the Quantacount and exposed to a known fluence of photoreactivating light at the wavelength of interest. After each irradiation a 25-μL sample was removed as described above and placed in the dark. The spectrum was monitored after the removal of each sample to ascertain that FADH$_2$ had not reoxidized during sampling. The sample in the second cuvette was photoreactivated in a manner identical with that of the first except that the sixth 25-μL sample was photoreactivated to completion by exposure to more than 50 000 erg mm^{-2}.

(*B*) *Far-UV.* Photoreactivation using far-UV wavelengths (254–280 nm) was carried out with E-FADH$_2$-MTHF in a manner similar to that of the near-UV–visible experiments. However, because many of the reaction components were highly absorbing in the far-UV region, photoreactivation had to be carried out under somewhat different conditions than for measurements in the near-UV–visible region. Components of the reaction mixture which absorbed strongly in the far-UV region had to be reduced or eliminated so that a 500-μL reaction mixture contained 1.72 μM photolyase, 10 mM DTT, 0.6% lactate, 1.5 μL of Oxyrase, and no BSA. The salt concentrations were unaltered. It was found that with the lowered Oxyrase/lactate concentration, the enzyme underwent oxidation when the syringe was inserted to withdraw sample. For this reason samples for each data point were deoxygenated, photoreduced, and photoreactivated individually. Except for these modifications, the procedure was the same as for the near-UV–visible experiments.

Analysis of Reaction Products. The extent of repair was quantified by either a T4 endo V nicking assay or a photolyase gel retardation method (Husain & Sancar, 1987). Since the reaction mixtures contained more than 1000-fold excess photolyase over substrate which interferes with both assays, we first purified away the DNA by extracting with phenol and ether followed by ethanol precipitation.

T4 endo V, which is specific for pyrimidine dimers, cleaves the glycosylic bond of the 5′-thymine of T<>T as well as the intradimer phosphodiester bond. With the 48-mer substrate this cleavage generates two radiolabeled 24-mers. The T4 endo V assay was conducted as follows: the photoreactivated DNA was resuspended in 12 μL of 10 mM Tris-HCl, pH 7.4, 10 mM NaCl, and 1 mM EDTA. To each sample was added an 8-μL mixture consisting of 2 μL of T4 endo V, 2 μL of 10 mM DTT, 2 μL of 1 mg/mL bovine serum albumin, and 2 μL of 10-fold concentrated T4 reaction buffer salts (0.5 M Tris-HCl, pH 8.0, 1 M NaCl, 10 mM EDTA). The samples were incubated at 37 °C for 30 min, lyophilized, resuspended in 10 μL of formamide containing 0.05% bromophenol blue and 0.05% xylene cyanol, and loaded onto a 12% sequencing gel. The gel was then autoradiographed (Figure 1), and the bands corresponding to full-length (repaired) and incised DNA were excised and quantified by Cerenkov counting.

The gel retardation assay is based on the fact that photolyase–DNA complexes migrate slower than uncomplexed DNA on native polyacrylamide gels (Husain & Sancar, 1987). For quantum yield measurements the assay was conducted as follows: reaction mixture (25 μL) containing approximately 0.05 nM photoreactivated DNA (20-mer) and 150 nM photolyase in photolyase buffer with 4% glycerol was incubated at room temperature in the dark to allow binding equilibrium to occur. The large molar excess of photolyase and the relatively high binding constant ($K_D = 10^{-8}$–10^{-9} M) of the enzyme ensure that all substrate would be bound under these assay

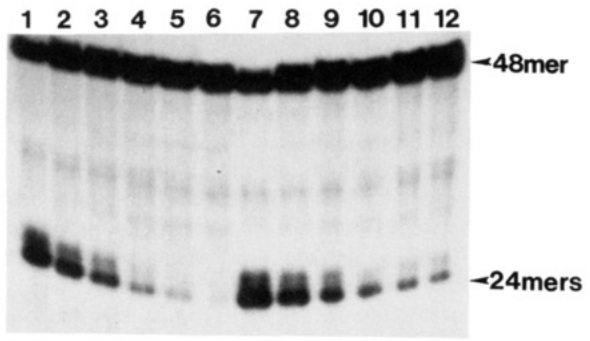

FIGURE 1: Coupled enzyme assay for photoreactivation. Photolyase–48-mer (T<>T) mixtures were exposed to various photoreactivating light fluences at 405 nm. The DNA was extracted with phenol and treated with T4 endo V. The reaction products were separated on a 12% sequencing gel. The 48-mer represents the T<>T strand that has been repaired as well as the complementary, nonsubstrate strand. The 24-mers are the two fragments produced by T4 endo V incision of the T<>T strand. The photoreactivation doses were as follows (erg mm^{-2}): lanes 1 and 7, none; lanes 2 and 8, 3750; lanes 3 and 9, 7500; lanes 4 and 10, 11 250; lanes 5 and 11, 15 000; lane 12, 18 750; lane 6, >50 000 for complete photoreactivation.

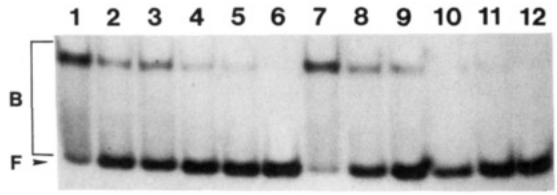

FIGURE 2: Analysis of T<>T photorepair by gel retardation assay. Photolyase–20-mer (T<>T) mixtures were exposed to 405-nm light of varying fluences and then separated on a 5% native polyacrylamide gel. The light fluences were as follows (erg mm^{-2}): lanes 1 and 7, none; lanes 2 and 8, 3000; lanes 3 and 9, 6000; lanes 4 and 10, 9000; lanes 5 and 11, 12 000; lane 12, 15 000. Lane 6, complete photoreactivation by exposure to >50 000 erg mm^{-2}. F, free DNA; B, bound DNA. The efficiency of retardation in the absence of repair is approximately 80% as is apparent by the "free DNA" band in lanes 1 and 7. This is corrected for when the percent substrate repaired is calculated.

conditions. The samples are applied to a 5% native polyacrylamide gel and electrophoresed at a constant voltage of 110 V for 40 min. Following electrophoresis the gel was subjected to autoradiography. A typical autoradiograph of a gel retardation experiment is shown in Figure 2. Because of the relatively high off-rate of the complex, *E. coli* photolyase does not yield a sharp band in gel retardation experiments. Instead, a "smear" is produced between the retarded band and the unretarded band. The bound fraction is taken to be the retarded band plus the smear between the two bands (Husain & Sancar, 1987). The radioactivity in various sections of the gel is determined by Cerenkov counting, and the fraction of free DNA is assumed to represent repaired DNA.

Data Analysis. The data from either assay were expressed as fraction of T<>T remaining unrepaired after each photoreactivating light dose for analysis by Rupert plot (Sancar et al., 1987). Under enzyme excess (E ≫ S) and light-limiting conditions the rate of photoreactivation can be described by the pseudo-first-order rate equation $d[ES]/dt = k_p I[ES]$, where $I dt$ is the differential of the light dose (dL) passing through the sample and corrected for absorption (Morowitz, 1951) and k_p is the photolysis constant (Harm & Rupert, 1970). Integration generates the equation used by Rupert plot: $\ln([ES]_t/[ES]_0) = -k_p L$. Thus, a plot of the natural log of the fraction of T<>T remaining at time t (after irradiation with monochromatic light of limiting intensity) versus light dose (fluence in erg mm^{-2}) yields a line with a slope equal to $-k_p$. Using k_p, $\epsilon\phi$, the photolytic cross section (T<>T repaired per incident photon), can be calculated (Rupert, 1962) from

$$\epsilon\phi\ (M^{-1}\ cm^{-1}) = (5.2 \times 10^9) k_p\ (mm^2\ erg^{-1}) \lambda^{-1}\ (nm) \quad (1)$$

where ϵ is the molar extinction coefficient (of ES complex and is taken to be equal to ϵ of photolyase because the absorption spectrum does not change upon binding) and ϕ is the quantum yield of photorepair (T<>T repaired per photon absorbed).

The molar extinction coefficients for E-$FADH_2$ and E-$FADH_2$-MTHF in the 340–435-nm range were determined with the published extinction coefficient $\epsilon_{450}(FAD_{ox})$ = 11 300 $M^{-1}\ cm^{-1}$ (Walsh, 1980) as reference. The E-$FADH_2$ and E-$FADH_2$-MTHF forms of the enzyme were prepared as described and the spectra recorded. Sodium dodecyl sulfate (0.77%) was then added to the enzyme preparations to denature the enzyme and convert $FADH_2$ to free FAD_{ox} and MTHF to free 10-formylfolate, which does not absorb at λ > 300 nm. From the absorption spectrum of FAD_{ox} the concentrations of the chromophores and their enzyme-bound extinction coefficients were calculated on the basis of absorbance values before addition of sodium dodecyl sulfate.

Photolytic Cross Section ($\epsilon\phi$) in Vivo. *E. coli* CSR603 (*recA1 uvrA6 phr-1*)/FlacI^q/pMS969 cells were grown overnight in Luria broth, collected, washed, and resuspended in phosphate-buffered saline (PBS) at a density of about 5×10^6 cells/mL and then irradiated with 2 erg mm^{-2} of 254-nm light to produce approximately 13 dimers per genome. These cells are totally deficient in DNA repair when kept in the dark and are therefore inactivated by single-hit kinetics. The cells were placed in a cuvette (1 mL) and exposed to photoreactivating light in the Quantacount as was done with DNA–photolyase mixtures (fluence rate 9.7 erg $mm^{-2}\ s^{-1}$). Samples were taken after predetermined light doses, and the cells were plated on Luria plates containing 20 μg/mL tetracycline after appropriate dilutions. From the increase in survival, the fraction of dimers repaired was calculated by assuming a Poisson distribution of dimers. The cells contain about 1000 photolyase molecules per cell, and therefore, at any given moment all dimers are bound by the enzyme as was found by single-flash photolysis (data not shown). Under these conditions the rate of repair is pseudo first order when light is limiting, and therefore, the data can be analyzed by Rupert plot as in the in vitro experiments (Harm et al., 1970).

RESULTS

Status of the Chromophores during Photoreactivation. *E. coli* photolyase, which is thought to contain stoichiometric amounts of $FADH_2$ and MTHF in vivo, loses 50–70% of its MTHF during purification, and its tightly bound $FADH_2$ becomes oxidized to $FADH^0$ (Payne et al., 1987; Johnson et al., 1988). To obtain the quantum yield of the physiological form of the enzyme, we wished to conduct photoreactivation experiments with enzyme having a full complement of both chromophores and with the flavin in the fully reduced state. The flavin can be photochemically reduced to $FADH_2$ in the presence of electron donors such as dithiothreitol (Heelis & Sancar, 1986).

Initially, we conducted our photorepair experiments by photoreducing deoxygenated E-$FADH^0$ or E-$FADH^0$-MTHF and transferring it to a deoxygenated reaction mixture containing substrate using a gas-tight syringe. The results obtained for both forms of enzyme were erratic, suggesting that MTHF did not contribute to repair and that $FADH_2$ was reoxidizing during the experiment. In addition, S. Hamm-Alvarez (personal communication) showed that photorepair with E-$FADH^0$-MTHF at nanomolar concentrations was more

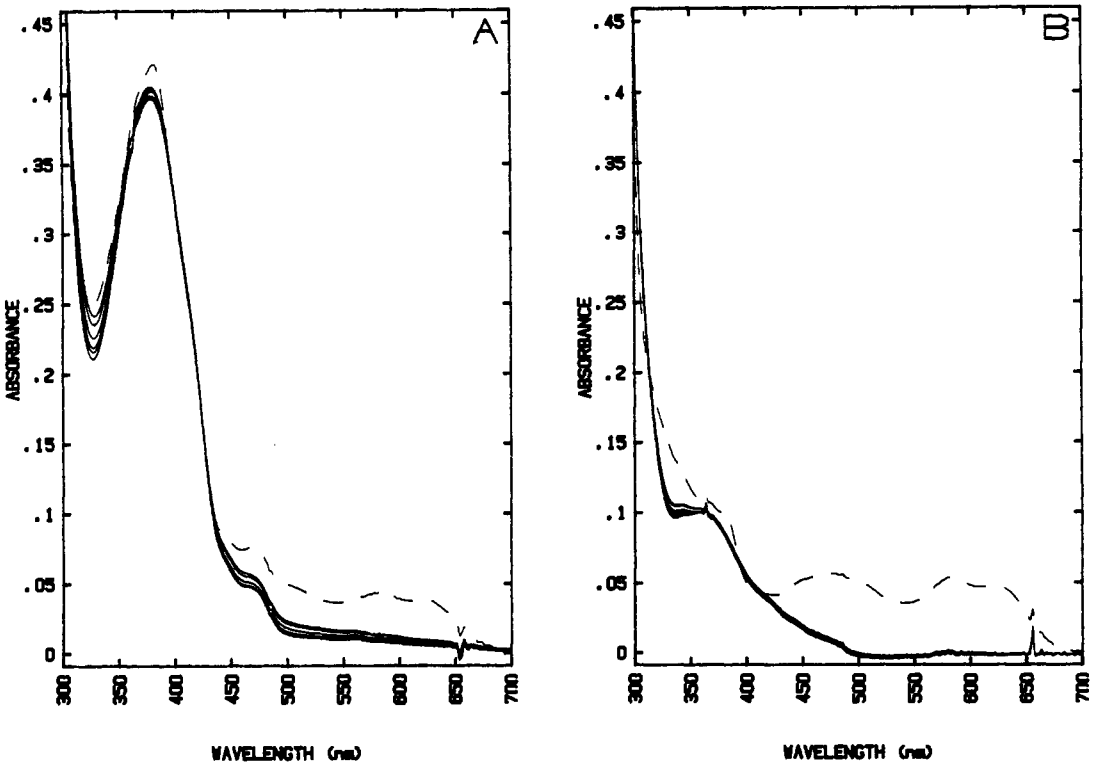

FIGURE 3: Photolyase absorption spectrum during action spectrum measurements. Either (A) E-FADH^0-MTHF or (B) E-FADH^0 was mixed with substrate, deoxygenated, and photoreduced. (--) Spectra before photoreduction; (—) spectra after photoreduction and subsequent sample removal after irradiation with various doses of 405-nm light.

efficient in the presence of excess MTHF, suggesting that MTHF may dissociate from the enzyme when diluted. For these reasons we decided to conduct photorepair experiments with micromolar concentrations of both forms of photolyase to monitor the status of the chromophores spectrophotometrically during the reaction. We found that while MTHF remained stable at these concentrations, the $FADH_2$ reoxidized during the transfer of enzyme to substrate. To avoid this problem, subsequent experiments were conducted by mixing enzyme and substrate in an anaerobic cuvette, deoxygenating the mixture, and photoreducing the enzyme with filtered (630-nm long pass) camera flashes. We have previously demonstrated that FADH^0, the only chromophore that absorbs at $\lambda > 630$ nm, does not promote photorepair or does so very inefficiently (Payne et al., 1987). Neither the photoreducing treatment nor the subsequent spectrophotometric measurements used to monitor the status of the chromophores cause any significant repair (data not shown), indicating that this procedure was appropriate for conducting quantum yield measurements. Typical absorption spectra of reaction mixtures containing E-$FADH_2$ and E-$FADH_2$-MTHF at micromolar concentration and substrate at nanomolar concentration taken during the course of photoreactivation experiments are shown in panels A and B of Figure 3, respectively. No measurable change occurred in the oxidation state of $FADH_2$ (no change in absorption at 580 nm) or in the association of MTHF with the apoenzyme (no change in absorption at 384 nm) during the course of the experiments, and thus, the photorepair efficiency of the two forms of the enzyme must reflect the contributions of one (E-$FADH_2$) or both (E-$FADH_2$-MTHF) chromophores.

Action Spectrum in the Near-UV. Photolytic cross-section ($\epsilon\phi$) measurements were conducted with enzyme containing $FADH_2$ alone and with a full complement of both chromphores to determine the role and efficiency of each chromophore in photorepair. Representative examples of the primary data in the form of Rupert plots [log (% T<>T remaining) vs fluence under enzyme excess conditions] are shown in Figure 4A for E-$FADH_2$ and in Figure 4B for E-$FADH_2$-MTHF. The photolytic cross sections obtained from these plots along with the extinction coefficients at the various wavelengths and the calculated quantum yields are tabulated in Table I. The absolute action spectra in the near-UV–visible region of the two forms were superimposed on their respective absorption spectra in Figure 5A,B. The absolute action spectrum of E-$FADH_2$ closely matches its absorption spectrum in the near-UV with an average quantum yield of $\phi_{ET} = 0.689 \pm$

Table I: Spectroscopic and Photochemical Parameters of Photolyase

enzyme	wavelength (nm)[a]	fluence rate (erg mm^{-2} s^{-1})	$\epsilon\phi$ (M^{-1} cm^{-1})	ϵ (M^{-1} cm^{-1})	ϕ
E-$FADH_2$	340	42.3	3336.1	4758	0.701
	355	41.0	3990.0	5572	0.716
	366	47.5	4770.8	5680	0.840
	384	56.1	2853.3	4556	0.626
	405	72.0	2086.3	3000	0.695
	420	74.6	1352.1	2217	0.610
	435	78.6	879.5	1382	0.636
E-$FADH_2$-MTHF	254[b]	24.4	66768.0		
	280[b]	73.7	17697.2		
		10.3			
	300[b]	27.3	5592.4		
	340	18.8	9577.6	15872	0.603
	355	10.7	15409.6	22052	0.699
	366	11.1	19463.4	26450	0.736
	384	13.6	14833.0	29501	0.503
	405	18.6	10718.1	22131	0.484
	420	33.3	7132.6	13905	0.513
	435	35.4	2237.3	3983	0.562

[a] In the region of 254–340 nm a Schott UG5 band-pass filter was used. In the region of 344–384 nm a Schott BG3 band-pass filter was used. In the region of 405–435 nm a Schott BG38 band-pass filter was used. [b] Accurate experimental values for ϵ in the 254–300-nm region are not available for the enzyme-bound chromophores.

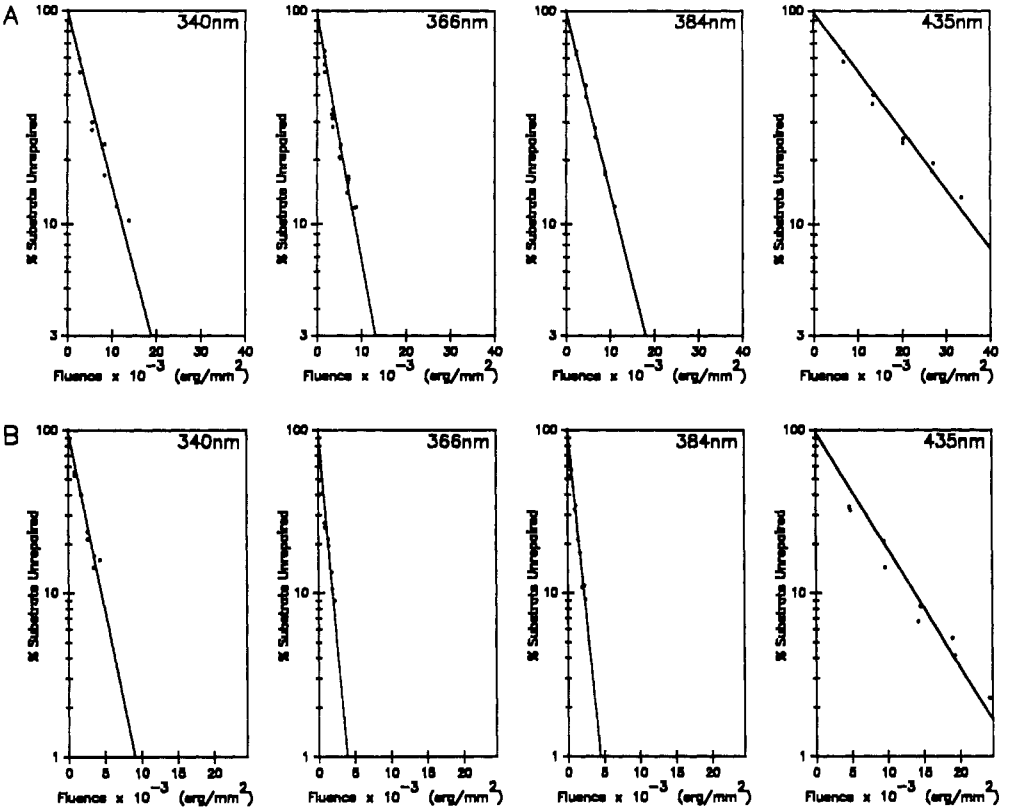

FIGURE 4: Rupert plots showing T<>T repair by E-$FADH_2$ and E-$FADH_2$-MTHF. The data points were obtained with the T4 endo V assay. The fluence rates ranged from 10 to 78 erg mm^{-2} s^{-1} and are listed in Table I.

0.072. The action spectrum of the E-$FADH_2$-MTHF form also matches fairly well its absorption spectrum, with an average quantum yield $\phi_{ET} = 0.589 \pm 0.091$. The close correspondence between the absorption spectrum of E-$FADH_2$-MTHF (which is dominated by the absorption of MTHF) and the absolute action spectrum suggests that upon excitation the two chromophores interact intimately, approaching the behavior expected of one chromophore. Indeed, if $FADH_2$ is considered to be the primary electron-transferring chromophore and MTHF to function via simple energy transfer, MTHF converts 80% of absorbed photons to excite $FADH_2$ for dimer repair:

$$\epsilon\phi(\text{E-FADH}_2\text{-MTHF}) = \epsilon(\text{FADH}_2)\phi_{ET}(\text{FADH}_2) + \epsilon(\text{MTHF})\phi_{\epsilon T}(\text{MTHF})\phi_{ET}(\text{FADH}_2) \quad (2)$$

By use of $\epsilon\phi(FADH_2)$, $\epsilon\phi$(E-$FADH_2$-MTHF), $\phi(FADH_2)$, and ϵ(MTHF) at various wavelengths, an average energy transfer quantum yield of $\phi_{\epsilon T}(MTHF) = 0.805$ is calculated (Table II). Alternatively, if MTHF behaves as an independent electron-transferring chromophore, $\phi_{ET}(MTHF) = 0.556$. However, it must be noted that while the agreement between the absorption spectrum of E-$FADH_2$ and its action spectrum is quite close, that of E-$FADH_2$-MTHF somewhat deviates in the 380–400-nm region. This might be a reflection of some unusual feature of the interactions between the two chromophores and will be addressed further under Discussion.

E-$FADH_2$-MTHF Is the Physiological Form of Photolyase. The results we have obtained so far combined with previous reports (Harm et al., 1970; Sancar et al., 1987a) on the photolytic cross section ($\epsilon\phi$) in vivo suggest that E-$FADH_2$-MTHF is the physiological form of the enzyme. To confirm that this form is, in fact, the in vivo form of the enzyme, we measured $\epsilon\phi_{384}$ on whole cells using experimental conditions very similar to those used for in vitro measurement except that they were conducted under aerobic conditions. The results of in vivo and in vitro measurements are shown in the form of a Rupert plot in Figure 6. The data points are nearly superimposable in the range of up to 70% repair, strongly suggesting that E-$FADH_2$-MTHF is indeed the in vivo form of photolyase. The divergence between in vivo and in vitro repair in the range of 70–90% repair suggests that the enzyme is slightly less stable in vitro than in vivo due to unknown factors.

Table II: Energy Transfer from MTHF to $FADH_2$

λ	ε(MTHF)	φ(MTHF)[a]	$\phi_{\epsilon T}$(MTHF)[a]
340	11493	0.543	0.775
355	16480	0.693	0.968
366	20770	0.707	0.842
384	24945	0.480	0.767
405	19131	0.451	0.649
420	11688	0.495	0.811
435	2601	0.522	0.821
av			0.805 ± 0.089

[a] These values were calculated with $\phi(FADH_2)$ determined at each wavelength.

Photoreactivation in the Far-UV. Photoreactivation was originally defined as the reversal of the effect of UV by exposure to longer wavelength radiation (Jagger, 1958). Nevertheless, the absorption spectrum of the chromophores extends into the short-wavelength region of the spectrum, and therefore, it is to be expected that the enzyme would catalyze repair of DNA upon excitation with short-wavelength UV. However, short-wavelength UV produces pyrimidine dimers with relatively high quantum yield ($\phi \sim 0.015$; Patrick & Rahn, 1976). Thus, in a photoreactivation assay with short-UV irradiation, pyrimidine dimers are continuously being formed as they are repaired by photolyase. Therefore, it is difficult, if not impossible, to demonstrate repair with most assays used for photolyase. The short oligomer duplexes used in our studies

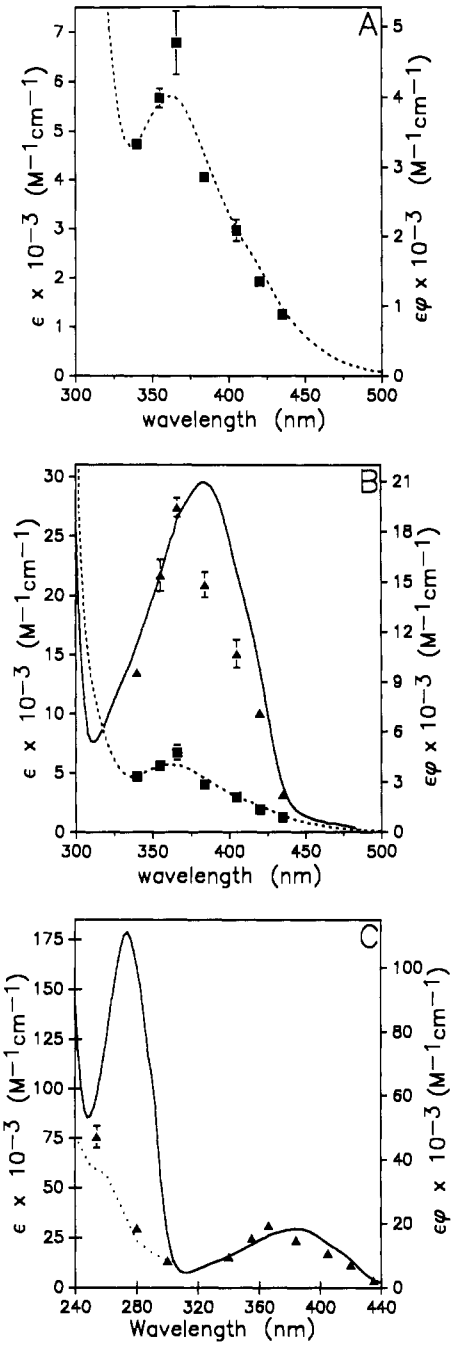

FIGURE 5: Absorption and absolute action spectra of E-FADH$_2$ and E-FADH$_2$-MTHF: (A) E-FADH$_2$ in the near-UV–visible range; (B) both E-FADH$_2$ and E-FADH$_2$-MTHF in the near-UV–visible range; (C) E-FADH$_2$-MTHF in the far-UV–visible range. The photolytic cross sections ($\epsilon\phi$) were calculated from the Rupert plots (examples of which appear in Figure 4). (■) $\epsilon\phi$ of E-FADH$_2$; (▲) $\epsilon\phi$ of E-FADH$_2$-MTHF; (—) absorption spectrum of E-FADH$_2$-MTHF; (--) absorption spectrum of E-FADH$_2$; (···) calculated absorption spectrum in the far-UV of FADH$_2$ plus MTHF based on the absorption spectra of the free chromophores.

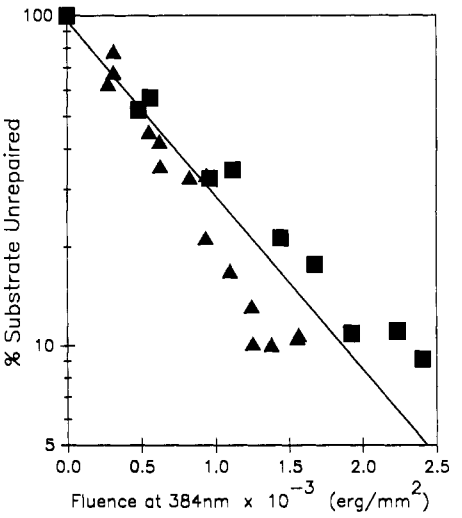

FIGURE 6: Rupert plot showing in vitro and in vivo repair at 384 nm. The fraction of dimers (in vitro) or photorepairable lesions (in vivo) remaining as a function of photoreactivating light fluence at 384 nm is plotted for (■) E-FADH$_2$-MTHF and (▲) photolyase-overproducing cells. The fluence rates for the in vitro and in vivo experiments were 13.6 and 10.3 erg mm^{-2} s^{-1}, respectively.

make it possible to conduct such experiments provided that the proper corrections are made for induction of pyrimidine dimers by short UV with $\phi \sim 0.015$ and direct reveral of photodimers with a quantum yield $\phi \sim 0.8$ (Setlow, 1966; Patrick & Rahn, 1976). The results of our photoreactivation experiments with short UV are summarized in Table I. The contribution of direct photoreversal was minor (~5% at the highest fluence) because even though the quantum yield of nonenzymatic photoreversal is high ($\phi \sim 0.8$) the dimer extinction coefficient is very low ($\epsilon_{254} = 300$ M^{-1} cm^{-1}) compared to that of the enzyme's chromophores. Similarly, dimer production in the substrate at the highest photoreactivating dose was undetectable because even though the extinction coefficient of pyrimidines at these wavelengths is reasonably high ($\epsilon \sim 8000$ M^{-1} cm^{-1}) the quantum yield of formation is quite low ($\phi \sim 0.015$). In Figure 5C the absolute action spectrum of photolyase in the 240–440-nm range is superimposed over the absorption spectrum of the enzyme. As is evident the match between the two spectra is close in the 300–440-nm region. At 280 and 254 nm the two diverge because the absorption spectrum in this range is dominated by the absorption of the aromatic residues of the protein. When the combined absorption spectrum of the two free chromophores is plotted (Figure 5C, dotted line), then the absorption spectrum matches the action spectrum reasonably well even in the short-wavelength region. Thus, it appears that the two chromophores function as photosensitizers in the far-UV as well as in the near-UV–visible region. Furthermore, these data indicate that the aromatic residues of the apoenzyme do not contribute to photorepair. This is interesting in view of the fact that the tripeptide Lys-Trp-Lys catalyzes photodimer reversal with $\lambda \geq 300$ nm (Helene & Charlier, 1971) and that antibodies raised against pyrimidine dimers which effectively reverse pyrimidine dimers with $\lambda \geq 300$ nm appear to contain a photosensitizing tryptophan at the binding site (Cochran et al., 1988). It must be noted, however, that a single tryptophan residue at the active site of photolyase contributing to photoreactivation with a quantum yield of $\phi \sim 0.5$ would add only $\epsilon\phi \sim 2500$ M^{-1} cm^{-1} to the photolytic cross section at 280 nm, and such a small difference would not be easily detectable with our assay.

Effect of DNA Primary and Secondary Structure on Photolysis. Previous research has shown that the rate of repair of pyrimidine dimers depends on the secondary structure of DNA, the type of the dimer, and the neighboring sequences in which a particular dimer is embedded. Thus, T<>T in poly(dA-dT) and C<>C in poly(dG-dC) are repaired by the yeast enzyme (which is structurally similar to the *E. coli* enzyme) with about $^1/_{15}$ the quantum yields of the same photodimers in natural DNA, presumably because of the unique secondary structures of the homopolymers (Rupert & To, 1976). Similarly, in *E. coli* cells T<>T is repaired 2-fold

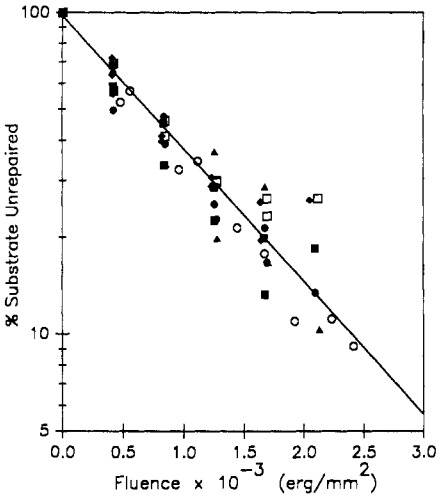

FIGURE 7: Rupert plot for repair at 384 nm by E-$FADH_2$-MTHF of T<>T substrates in various sequence contexts: (○) 48-mer; (●) 20-mer A; (▲) 20 mer B; (■) 20-mer C; (◆) 20-mer D; (□) single-stranded 48-mer. The fluence rates in these experiments ranged from 13.6 to 15.0 erg mm^{-2} s^{-1}.

faster than T<>C which is in turn repaired 2-fold faster than C<>C (Setlow & Carrier, 1966). In addition, yeast photolyase shows biphasic kinetics in Rupert plots with natural DNA containing exclusively T<>T (prepared by acetophenone photosensitization), indicating that sequence context affects the quantum yield (Rupert, 1975). Myles et al. (1987) also observed different rates of repair with *E. coli* photolyase in a manner dependent on neighboring sequence and type of photodimers. At present we are unable to address all the issues regarding the effects of DNA structure on the photochemistry of photolyase. However, we have been able to address two of these issues: the effect of single strandedness and neighboring sequences on the quantum yield.

To assess the effect of single strandedness on the photochemical reaction, we conducted photolytic cross-section ($\epsilon\phi$) measurements on heat-denatured 48-mer substrate. Figure 7 shows that T<>T is repaired with the same quantum yield in single- and double-stranded substrates. Thus, we conclude that strandedness of DNA has no effect on the binding of photolyase to DNA (Sancar et al., 1985) or on the efficiency of the photocatalytic step.

To evaluate the effect of neighboring sequences on the photochemistry of the reaction, we used, in addition to the 48-mer, four different 20-bp duplexes containing a single T<>T as substrate. The data of photoreactivation experiments with these substrates are also shown in Figure 7, and the results are summarized in Figure 8. As is apparent from these figures, all substrates are repaired with essentially the same quantum yield. Note that the T<>T in the 48-mer is in a relatively GC-rich sequence, GT<>TGG, yet it is repaired with the same efficiency as a T<>T in an AT-rich sequence, AAT<>TA. Thus, we conclude, within the limitation imposed by our limited substrate repertoire, that for a given type of dimer the photochemical repair efficiency is not influenced by the immediate neighboring sequence.

Status of Chromophores after Catalysis. As all of the experimental data presented thus far were acquired under conditions of enzyme excess over substrate, it is possible that the measured repair efficiencies represent only those for one round of repair rather than catalytic repair. It could be argued that each round of catalysis results in degradation, dissociation, or irreversible change of one or both chromophores. To investigate the status of the chromophores after several rounds of catalysis, we mixed E-$FADH_2$-MTHF with about 5-fold excess T<>T in oligo$(dT)_{15}$ and carried out the photoreactivation at 384 nm under anaerobic conditions. During the photoreactivation treatment the status of the chromophores was monitored spectrophotometrically, and the extent of repair was determined by the disappearance of T<>T from a radiolabeled 48-mer duplex which was included in the reaction mixture as a tracer. The results shown in Figure 9 indicate that the spectroscopic properties of the enzyme do not change after five rounds of photocatalytic cycles. Thus, from these data we can conclude that the chromophores remain intact under turnover conditions, suggesting that the quantum yields determined under enzyme-saturating conditions accurately represent true catalytic efficiency. In fact, a calculation of the quantum yield from K_{cat} obtained in this experiment gives $\phi_{384} = 0.503$, in agreement with $\phi_{384} = 0.503$ obtained under non-turnover conditions. (Also note that the fact that the near-UV–visible spectrum remains the same before and after repair of the substrate indicates that DNA binding has no effect on the near-UV absorption spectrum of photolyase.)

Protection of Photolyase from Oxidation by Substrate. During quantum yield measurements with spectrophotometrically detectable concentrations of E-$FADH_2$ we noticed that the enzyme-bound $FADH_2$ was extremely susceptible to oxidation by trace amounts of oxygen as evidenced by the appearance of the characteristic radical absorption in the 450–700-nm region. However, to our surprise, quantum yield measurements conducted under conditions where reoxidation of $FADH_2$ was observed yielded values significantly higher

Substrate	Length	Φ_{384}
5'-...GCAGGCAAGT<>TGGAGGAATT... 3'-...CGTCCGTTCA--ACCTCCTTAA...	48 bp	0.503 ± 0.026
5'-GCAGCTGACGAAT<>TTAGCTC 3'-GACTGGTTA--AATCGAGCTCG	20 bp (A)	0.489 ± 0.041
5'-GCTCGAGCTCAAT<>TAGTCAG 3'-CTCGAGTTA--ATCAGTCCTCG	20 bp (B)	0.478 ± 0.079
5'-GCAGCTGACTAAT<>TGAGCTC 3'-GACTGATTA--ACTCGAGCTCG	20 bp (C)	0.504 ± 0.061
5'-GCTCGAGCTAT<>TAACGTCAG 3'-CTCGATA--ATTGCAGTCGACG	20 bp (D)	0.449 ± 0.022
5'...GCAGGCAAGT<>TGGAGGAATT...	48 bases	0.429 ± 0.030

FIGURE 8: Effect of strandedness and neighboring sequence on quantum yield of repair by E-$FADH_2$-MTHF. The quantum yields were calculated from the Rupert plots shown in Figure 7 with ϵ_{384} = 29 501 M^{-1} cm^{-1}. Only part of the sequence of the 48-mer substrates is shown.

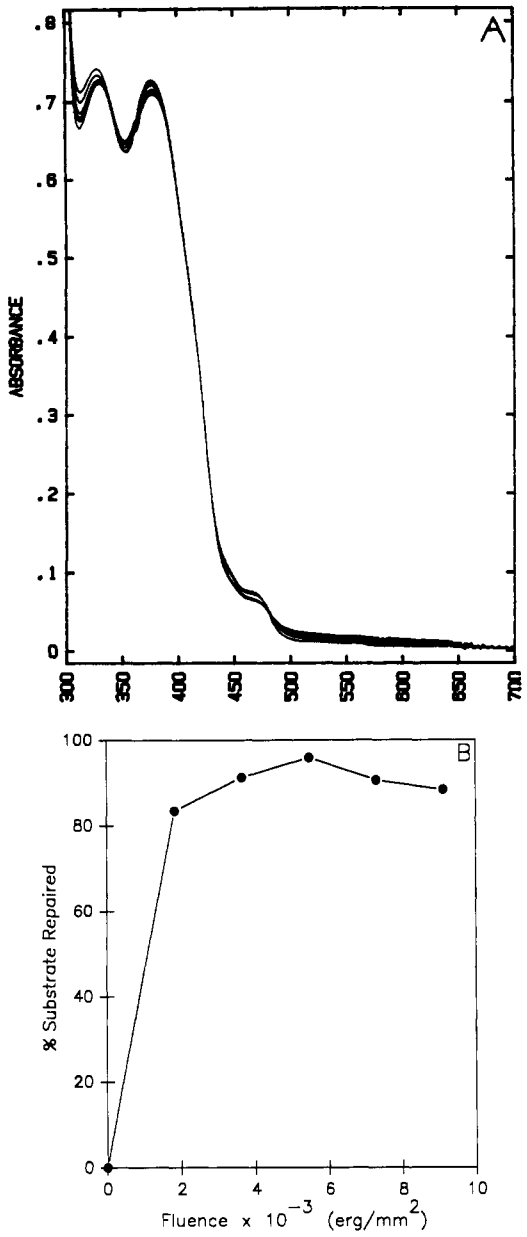

FIGURE 9: Effect of several rounds of repair on photolyase spectrum. Photolyase was mixed with a 5-fold excess T<>T in oligo(dT)$_{15}$ and then photoreduced anaerobically followed by photoreactivation at 384 nm. (A) Spectra were taken after 0, 4000, 8000, 12000, 16000, and 20000 erg mm^{-2} at a fluence rate of 56.5 erg mm^{-2} s^{-1}. The peak at 320 nm is due to the 6–4 photoproduct present in the T<>T substrate (Patrick & Rahn, 1976). This photoproduct is not repaired by photolyase (Brash et al., 1985). (B) Samples were taken at each irradiation point, and the level of repair of the 48-mer tracer was quantified by T4 endo V assay.

(ϕ_{384} = 0.52) than those obtained with E-FADH^0 under aerobic conditions without prior photoreduction (ϕ_{384} = 0.14).

These observations suggested the possibility that although rapid oxidation of E-FADH$_2$ occurred, the reduced enzyme that bound substrate remained reduced while free enzyme (90–95% of the enzyme in the reaction mixture) became oxidized to E-FADH^0. To test whether substrate binding inhibits oxidation of enzyme-bound FADH$_2$, we photoreduced E-FADH^0-MTHF to E-FADH$_2$-MTHF under anaerobic conditions in photolyase buffer (omitting the oxygen-scavenging Oxyrase/lactate system), in the presence and absence of a 10-fold molar excess of T<>T in oligo(dT)$_{15}$. Upon completion of photoreduction, indicated by the loss of 450–700-nm absorption, the cuvettes were warmed to room temperature,

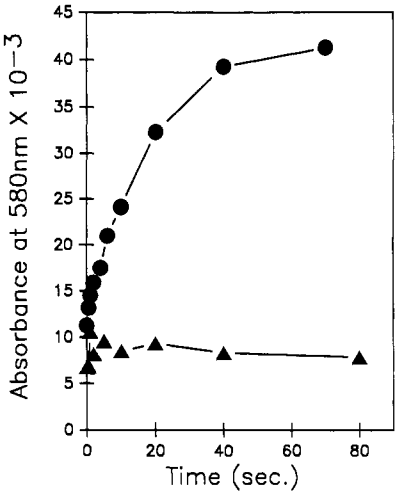

FIGURE 10: Protection of FADH$_2$ from air oxidation by substrate. Enzyme (●) or enzyme–substrate (▲) mixtures were photoreduced anaerobically and then exposed to air, and the increase in absorbance at 580 nm was monitored as an indicator of FADH$_2$ oxidation to FADH^0.

and the contents were exposed to air. The increase in absorption at 580 nm was monitored over a period of 80 min as an indicator of FADH$_2$ reoxidation to FADH^0. The results are shown in Figure 10. As apparent from this plot in the presence of excess substrate, no measurable reoxidation to FADH^0 occurs, while in the absence of substrate FADH$_2$ reoxidation occurs with a pseudo-first-order rate constant k = 6.3 × 10^{-4} s^{-1} in agreement with earlier results on reoxidation of E-FADH$_2$ to E-FADH^0 (Heelis et al., 1987). Thus, from these experiments we conclude that substrate binding protects the enzyme-bound FADH$_2$ from oxidation. We think this protection is specific for the DNA binding site in contrast to stabilization of the entire protein against heat denaturation (Sancar & Sancar, 1984). N5 of FADH$_2$, which is oxidized upon exposure to O_2, is the atom most likely to be the electron donor to Pyr<>Pyr substrate. Therefore, it is expected that this position would be protected from the solvent upon formation of the enzyme–substrate complex and, thus, be resistant to oxidation.

Effect of Anaerobiosis on Photolyases. The extreme susceptibility of purified *E. coli* photolyase to air oxidation, resulting in conversion of FADH$_2$ to the catalytically inert FADH^0, necessitated that all quantum yield measurements be conducted anaerobically. As repair of Pyr<>Pyr most likely involves a redox reaction, it could be argued that the enzyme has a different quantum yield under aerobic conditions. To investigate whether anaerobiosis has any effect on the photochemical reaction catalyzed by photolyases, we conducted photoreactivation kinetics with two other photolyases under anaerobic conditions and compared the quantum yields obtained in these experiments to those obtained under aerobic conditions for the same enzymes. Yeast photolyase, like *E. coli* photolyase, contains MTHF and FADH$_2$, but in contrast to the *E. coli* enzyme, its FADH$_2$ cofactor is resistant to air oxidation during purification (Sancar et al., 1987b). Thus, anaerobiosis is not required to maintain FADH$_2$ with this enzyme. *Methanobacterium thermoautotrophicum* belongs to the deazaflavin class of photolyases, and it is presumed to have an FADH$_2$ cofactor in addition to the 8-hydroxy-5-deazaflavin chromophore (Kiener et al., 1989). The FADH$_2$ chromophore of this enzyme must be somewhat resistant to air oxidation because the near-UV–visible absorption spectrum of the enzyme is typical of 5-deazaflavin with only a small

Table III: Photoreactivation Efficiences of Various Photolyases under Anaerobic and Aerobic Conditions

photolyase	class	λ_{max} (nm)	$\epsilon\phi$		ϕ		relative photoreactivation efficiency in sunlight[a]
			aerobic	anaerobic	aerobic	anaerobic	
E. coli	folate	384	19778.2[b]	14833.0	0.670[c]	0.503	0.41
S. cerevisiae	folate	377	13630.0[d]	11994.0	0.490[d]	0.427	0.30
M. thermoautotrophicum	deazaflavin	440	17508.4[e]	14483.0[e]	0.438[e]	0.362[e]	1.0

[a] These values were calculated by multiplying the experimentally determined photolytic cross section ($\epsilon\phi$) by the relative sunlight irradiance (Wurtman, 1975). [b] Measurements performed in vivo. [c] ϕ is calculated by assuming ϵ_{384} (in vivo) = 29501 M^{-1} cm^{-1}. [d] G. Sancar (personal communication). [e] These values are somewhat higher than those reported by Kiener et al. (1989) possibly because the enzyme used in that study contained some $FADH^0$.

absorption peak in the area corresponding to flavin radical. The quantum yields of these enzymes under aerobic and anaerobic conditions along with some other relevant photochemical properties are listed in Table III. As is apparent from this table, anaerobiosis has no effect on the quantum yields of these photolyases. Therefore, the stringent anaerobiosis, required to obtain repair at high quantum yield with the *E. coli* photolyase, is simply for maintaining the enzyme in its reduced (physiological) form and has no effect on the efficiency of photoreactivation per se.

Discussion

In general, photochemical reactions proceed from the lowest excited state because the rate of internal conversion is very rapid ($\sim 10^{12}$ s^{-1}) compared to those of most chemical reactions (Turro et al., 1978). Thus, the absolute action spectrum of a photochemical process is expected to mimic the shape of the absorption spectrum, and consequently, the quantum yield of photochemical reactions does not vary with wavelengths. However, in a system with more than one chromophore the relationship between the action and absorption spectra may be more complex. Absolute quantum yield measurements in such systems may help define the roles of individual chromophores and often reveal some information regarding the mechanism of the primary photochemical reaction.

We previously published an absolute action spectrum of *E. coli* DNA photolyase (Sancar et al., 1987a). We obtained quantum yields ranging from 0.062 (at 384 nm) to 0.003 (at 625 nm). The E-$FADH^0$ form containing an indeterminate amount of MTHF was used in that study. The "second chromophore" was not identified at the time, and therefore, we were unaware that the enzyme purified by our standard procedure contained a substoichiometric amount of MTHF. Furthermore, later investigations (Payne et al., 1987) showed that the radical form was not the physiologically relevant form and that, in fact, the quantum yield measured in the 350–440-nm region was the quantum yield for photoreducing the nonactive radical form into the catalytically active $FADH_2$ form. The identification of the second chromophore as MTHF (Johnson et al., 1988) and the development of a simple procedure to supplement the purified enzyme with this cofactor (Hamm-Alvarez et al., 1989) have enabled us to prepare enzyme of well-defined chromophore content for the first time.

The near-UV–visible action spectrum measurements described in this paper were done for three reasons. First, the ability to prepare enzyme completely devoid of MTHF and with stoichiometric amount of MTHF provided a unique opportunity for examination of the individual roles of the two chromophores. Second, photolytic cross-section measurements with photolyase-overproducing whole cells and with E-$FADH_2$-MTHF enabled us to test the premise that enzyme containing $FADH_2$ and a full complement of MTHF is the in vivo catalytically active form of the enzyme. Third, the ability to prepare enzyme of defined chromophore content and the development of an assay designed to monitor the status of both chromophores during photoreactivation have made it possible to obtain precise values for the quantum yield of various photochemical processes leading to dimer repair.

The near-UV–visible action spectrum of E-$FADH_2$ closely matched the absorption spectrum, which indicates that $FADH_2$ participates in a single-chromophore photocatalytic system and confirms earlier data indicating that MTHF is not required for Pyr<>Pyr repair (Heelis et al., 1987; Hamm-Alvarez et al., 1989). The similarity in shape of the absorption and action spectra indicates that this photochemical reaction occurs from the first excited singlet state of $FADH_2$. Consequently, the quantum yield of repair by electron transfer (ϕ_{ET}) is constant within the experimental error of our assay over the wavelengths measured with an average value of $\phi_{ET} = 0.689 \pm 0.072$. Thus, repair catalyzed by E-$FADH_2$ is extremely efficient.

It is of some surprise that the near-UV–visible action spectrum of E-$FADH_2$-MTHF is also quite similar to its absorption spectrum, yielding a fairly constant quantum yield of $\phi_{ET} = 0.589 \pm 0.091$. This indicates that MTHF also contributes to photosensitization with high efficiency and confirms previous data implicating MTHF in photorepair (Heelis et al., 1987; Hamm-Alvarez et al., 1989). Furthermore, the photolysis cross section obtained with E-$FADH_2$-MTHF closely matches the in vivo value (at 384 nm), providing strong evidence that this is the in vivo form of the enzyme.

The relationship between the action spectrum and the absorption spectrum of E-$FADH_2$-MTHF in the near-UV–visible region deserves further comment. The contribution to absorbance of the two chromophores over the 300–450-nm region is quantitatively different. The $FADH_2$ chromophore has a nearly symmetrical peak with a maximum at 366 nm (ϵ = 5680 M^{-1} cm^{-1}); MTHF has an absorption peak at 384 nm (ϵ = 26550 M^{-1} cm^{-1}). Thus, the contribution of the two chromophores to total absorbance is wavelength dependent. For example, at 384 nm 85% of the absorption is due to MTHF while this value is only 65% at 435 nm. If the two chromophores were to mediate photorepair independently and with significantly different quantum yields, $\epsilon\phi$ of E-$FADH_2$-MTHF would vary in a wavelength-dependent manner according to the varying relative contributions of the two chromophores to the overall absorption. Although we do see some wavelength dependence of the quantum yield (most notably at 366 nm), this fluctuation does not follow a pattern predicted from the chromophores' absorption spectra. Therefore, we conclude that, within the resolution of our assay, the quantum yield of E-$FADH_2$-MTHF is constant over the 330–435-nm region. There are several theoretical possibilities to explain this observation in a two-chromophore system: (i) the two chromophores repair dimer (by electron transfer) independently with relatively similar quantum yields; (ii) the

two chromophores act independently, but the MTHF functions only as an antenna transferring energy extremely efficiently to the $FADH_2$ which repairs dimers by electron transfer; (iii) the two chromophores interact and behave as one chromophore. We will consider each model briefly.

(i) We consider electron transfer from both chromophores very unlikely as MTHF is known to "transfer energy" to flavin very rapidly, in <40 ps (Heelis et al., 1990), and with very high quantum yield (Heelis et al., 1987). (ii) Efficient energy transfer from MTHF to $FADH_2$ by dipole–dipole interaction (Forster type) would seem unlikely, considering that the absorption peak of MTHF is 20-nm red-shifted relative to the absorption maximum of $FADH_2$, suggesting that energy transfer would be an endothermic reaction rather than the exothermic reaction required for high-efficiency energy transfer. (iii) A possible explanation for the action spectra data is one where the two chromophores interact in a manner approaching that of one chromophore. There is no evidence for interaction in the ground state as evidenced by the fact that MTHF has no effect on the absorption spectrum of $FADH^0$ (Hamm-Alvarez et al., 1989). Therefore, such an interaction must occur in the excited state. Indeed, a single transient species is detected at <40 ps by flash photolysis of E-$FADH^0$-MTHF (Heelis et al., 1990), which clearly has components of both chromophores. The excited species decays with a simple first-order rate constant, and the decay does not coincide with the formation of another species, ruling out a simple energy-transfer process. With all of these considerations we tentatively conclude that the repair by E-$FADH_2$-MTHF involves an exciplex formation. Perhaps, such a mechanism may also explain the significant and reproducible divergence between the absorption and action spectra of the holoenzyme at 366 nm. However, admittedly, exciplex is a rare phenomenon, and much more work is needed to prove such an unusual photobiological reaction. In fact, it has been suggested[2] that the fact that the action spectrum for E-$FADH_2$-MTHF is quite similar to the absorption spectrum of E-$FADH_2$ would rule out independent electron transfer by two chromophores and might well support energy transfer from MTHF to $FADH_2$ without having to invoke an exciplex. According to this view a Forster-type mechanism may not be applicable when the two chromophores are very close. In such a case, electron exchange or possibly some other mechanism may be operating at an exceedingly fast rate, quite possibly faster than vibrational relaxation. If the exchange is faster than vibrational relaxation, the shape of the action spectrum would be expected to be determined by the product of the absorption spectrum of E-MTHF and that of E-$FADH_2$. It could be debated that this explanation is a "semantic variant" of an exciplex (Creed & Caldwell, 1985).

Photolyases, as a class, are rich in aromatic amino acids, especially tryptophan. Therefore, demonstration of photoreactivation in the far-UV has some mechanistic significance as one or more of these residues may act as a "third chromophore". They could be involved in providing an aromatic shell around the chromophore to facilitate electron transfer such as seen in photosynthetic reaction centers (Deisenhofer & Michel, 1989) and in bacteriorhodopsin (Mogi et al., 1989). Alternatively, they could be involved in electron transfer directly as has been shown in model systems (Helene & Charlier, 1971; Van Camp et al., 1987) and in photoreversal of Pyr<>Pyr catalyzed by anti-Pyr<>Pyr antibodies (Cochran et al., 1988). However, if the photolyase tryptophans were contributing to repair, the apparent quantum yield at 280 nm (based on $FADH_2$ and MTHF absorption) would be expected to be higher than that seen at other wavelengths. As this is not observed, we conclude that photolyase tryptophan residues do not directly contribute to repair.

The far-UV photolytic cross-section measurements are also interesting because they demonstrate, for the first time, that the 254-nm wavelength used routinely for making photodimers is also very effective in photoreactivation. Previously, the shortest wavelength shown to catalyze photolyase mediated repair was 280 nm (Eker et al., 1986). These authors could not photoreactivate with shorter wavelengths because they used a biological assay (transformation) for repairing Pyr<>Pyr, and at shorter wavelengths more Pyr<>Pyr were introduced into the substrate than were repaired. By using a short DNA fragment with a single dimer, we have overcome the problems caused by other competing reactions (direct photoreversal, photodimerization) and have been able to demonstrate photoreactivation with 254 and 280 nm. Whether photoreactivation by these wavelengths has biological significance remains to be seen. A simple calculation shows that a cell containing a 10-kbp plasmid and about 1000 molecules of photolyase when irradiated with 10 erg mm^{-2} s^{-1} of 254 nm will repair photodimers as soon as they are formed. However, *E. coli* K12 cells contain only 10 molecules of photolyase. It is possible that other organisms have more photolyase than *E. coli* (Kiener et al., 1989), and thus, photoreactivation at 254 nm may contribute to survival.

The substrate also must be considered in any mechanistic study of photolyase. It has been known for some time that not all Pyr<>Pyr are repaired with equal efficiency (Setlow & Carrier, 1966) and that a given Pyr<>Pyr may be repaired with varying efficiencies depending on the DNA structural context (Rupert & To, 1976). Indeed, it was even proposed that the chromophore was created by a charge-transfer complex between the *E. coli* enzyme and its substrate (Cimino & Sutherland, 1982). We have compared the quantum yield for repairing T<>T in single- and double-stranded DNA and in several duplex sequence contexts. For all substrates tested, approximately the same quantum yield was obtained. Thus, we conclude that the substrate does not contribute to chromophore formation and, furthermore, the photochemical reaction for repairing T<>T is quite independent of the primary and secondary structures of DNA. This is not surprising as photolyase achieves specific recognition mainly by its interactions with the phosphodiester bonds in the damaged strand (Husain et al., 1987) and perhaps with the cyclobutane ring itself. However, it is known that some C<>C are quite resistant to photoreactivation (Myles et al., 1987). Therefore, we do expect to see some effect on the quantum yield of repair depending on the type of photodimer and the DNA structure as other dipyrimidines and other DNA structures are probed.

As all of the quantum yield experiments described in this paper were conducted under enzyme-excess conditions, it was necessary to demonstrate that several rounds of repair did not effect the chromophores or the quantum yield. Experiments with excess substrate, in which several turnovers occurred, indicated that the chromophores did not undergo any change. Furthermore, the quantum yield under turnover conditions is the same as that obtained under enzyme-excess conditions. Thus, the quantum yields measured under enzyme-excess conditions accurately represent the true catalytic efficiency of dimer repair.

E. coli photolyase is unique among photolyases in that during purification both of its chromophores undergo some

[2] We thank an anonymous referee for suggesting this alternative explanation of our data.

changes. The MTHF dissociates from the enzyme gradually while the $FADH_2$ becomes oxidized rapidly to $FADH^0$ and more slowly to FAD_{ox}. Because of these complications, special precautions were taken to ensure that the enzyme was maintained in the physiological form during quantum yield measurements. To prevent oxidation of $FADH_2$, measurements were conducted under anaerobic conditions. It was conceivable that a photochemical reaction which involves oxidation–reduction may proceed differently under anaerobic conditions. Therefore, we conducted photoreactivation experiments with two other photolyases, one of the folate class (yeast) and one of the deazaflavin class (methanogen), under anaerobic conditions and compared the quantum yields to those obtained aerobically. No significant difference was found. Thus, we conclude that the quantum yield obtained with *E. coli* photolyase represents the true photochemical reaction taking place in vivo under aerobic condition where the enzyme is somehow maintained in the E-$FADH_2$-MTHF form. What keeps the enzyme reduced in vivo is a matter of great interest and is currently under investigation.

Finally, accurate quantum yields for a number of photolyases are now available, and a comparison is in order. In Table III we have tabulated the photolytic cross sections of these three photolyases (representing the two classes of photolyase) in order to compare the relative efficiencies of these enzymes under natural conditions. The photolytic cross section combines two photochemical parameters, the extinction coefficient, which is a measure of the probability of an incident photon being absorbed, and the quantum yield, which is the measure of the probability of a given photochemical reaction occurring as a result of absorbing a photon. Thus, the photolytic cross section for a photolyase is a measure of the efficiency with which an incident photon is utilized to carry out photorepair. At the most effective wavelengths (370–390 nm) for *E. coli* and yeast photolyases, this value is 12 000–20 000 M^{-1} cm^{-1}, and for the methanogen enzyme (430–450 nm) the value is about 14 000–17 000 M^{-1} cm^{-1}. Since sunlight contains a 2–3-fold higher flux of photons at the 430–450-nm region of the spectrum compared to the 370–390-nm region (Wurtman, 1975) under natural conditions, the deazaflavin class of photolyases probably repair DNA at more than double the rate of the folate class.

Acknowledgments

We are grateful to S. Hamm-Alvarez and P. F. Heelis for providing the spectra of MTHF and $FADH_2$, to G. Sancar for yeast photolyase, to J. S. Taylor and D. Svoboda for the 20-mer substrates, and to C. Walsh for supplying us with the methanogen photolyase. N. Payne and M. Phillips provided excellent technical help.

Registry No. $FADH_2$, 1910-41-4; MTHF, 122642-16-4; DNA photolyase, 37290-70-3.

References

Brash, D. E., Franklin, W. A., Sancar, G. B., Sancar, A., & Haseltine, W. A. (1985) *J. Biol. Chem. 260*, 11438–11441.

Calvert, K. G., & Pitts, J. N., Jr. (1966) *Photochemistry*, pp 783–786, Wiley, New York.

Cimino, G. D., & Sutherland, J. C. (1982) *Biochemistry 21*, 3914–3921.

Cochran, A. G., Sugasawara, R., & Schultz, P. G. (1988) *J. Am. Chem. Soc. 110*, 7888–7890.

Creed, D., & Caldwell, R. A. (1985) *Photochem. Photobiol. 41*, 715–739.

Deisenhofer, J., & Michel, H. (1989) *EMBO J. 8*, 2149–2170.

Eker, A. P. M., Hessels, J. K. C., & Dekker, R. H. (1986) *Photochem. Photobiol. 44*, 197–205.

Hamm-Alvarez, S., Sancar, A., & Rajagopalan, K. V. (1989) *J. Biol. Chem. 264*, 9649–9656.

Harm, H., & Rupert, C. S. (1970) *Mutat. Res. 10*, 307–318.

Hatchard, C. G., & Parker, C. A. (1956) *Proc. R. Soc. London A235*, 518–536.

Heelis, P. F., & Sancar, A. (1986) *Biochemistry 25*, 8163–8166.

Heelis, P. F., Payne, G., & Sancar, A. (1987) *Biochemistry 26*, 4634–4640.

Heelis, P. F., Okamura, T., & Sancar, A. (1990) *Biochemistry 29*, 5694–5698.

Helene, C., & Charlier, M. (1971) *Biochem. Biophys. Res. Commun. 43*, 252–256.

Husain, I., & Sancar, A. (1987) *Nucleic Acids Res. 15*, 1109–1120.

Husain, I., & Sancar, G. B., Holbrook, S. R., & Sancar, A. (1987) *J. Biol. Chem. 262*, 13188–13197.

Husain, I., Griffith, J., & Sancar, A. (1988) *Proc. Natl. Acad. Sci. U.S.A. 85*, 2558–2562.

Jagger, J. (1958) *Bacteriol. Rev. 22*, 99–142.

Johnson, J. L., Hamm-Alvarez, S., Payne, G., Sancar, G. B., Rajagopalan, K. V., & Sancar, A. (1988) *Proc. Natl. Acad. Sci. U.S.A. 85*, 2046–2050.

Jorns, M. S., Sancar, G. B., & Sancar, A. (1984) *Biochemistry 23*, 2673–2679.

Kiener, A., Husain, I., Sancar, A., & Walsh, C. (1989) *J. Biol. Chem. 264*, 13880–13887.

Lamola, A. A. (1968) *Photochem. Photobiol. 8*, 601–616.

Massey, V., & Hemmerich, P. (1978) *Biochemistry 17*, 9–16.

Mogi, T., Marti, T., & Khorana, H. G. (1989) *J. Biol. Chem. 164*, 14197–14201.

Morowitz, H. J. (1950) *Science 111*, 229–230.

Myles, G. M., Van Houten, B. V., & Sancar, A. (1986) *Nucleic Acids Res. 15*, 1227–1243.

Patrick, M. H., & Rahn, R. D. (1976) in *Photochemistry and Photobiology of Nucleic Acids* (Wang, S. Y., Ed.) Vol. II, pp 35–145, Academic Press, New York.

Payne, G., Heelis, P. F., Rohrs, B. R., & Sancar, A. (1987) *Biochemistry 26*, 7121–7127.

Payne, G., Wills, M., Walsh, C. T., & Sancar, A. (1990) *Biochemistry 29*, 5706–5711.

Penefsky, M. S. (1977) *J. Biol. Chem. 151*, 2891–2899.

Rupert, C. S. (1962) *J. Gen. Physiol. 45*, 725–741.

Rupert, C. S., & To, K. (1976) *Photochem. Photobiol. 24*, 229–235.

Rupert, C. S., Harm, H., & To, K. (1975) *Ann. Brazil Acad. Sci. 45*, 151–159.

Sancar, A., & Sancar, G. B. (1984) *J. Mol. Biol. 172*, 223–227.

Sancar, A., & Sancar, G. B. (1988) *Annu. Rev. Biochem. 57*, 29–67.

Sancar, A., Smith, F. W., & Sancar, G. B. (1984) *J. Biol. Chem. 259*, 6028–6032.

Sancar, G. B., Smith, F. W., & Sancar, A. (1985) *Biochemistry 24*, 1849–1855.

Sancar, G. B., Jorns, M. S., Payne, G., Fluke, D. J., Rupert, C. S., & Sancar, A. (1987a) *J. Biol. Chem. 262*, 492–498.

Sancar, G. B., Smith, F. W., & Heelis, P. F. (1987b) *J. Biol. Chem. 262*, 15457–15465.

Setlow, R. B. (1966) *Science 153*, 379-386.
Setlow, R. B., & Carrier, W. L. (1966) *J. Mol. Biol. 17*, 237-254.
Turro, N. J., Ramamurthy, V., Cherry, W., & Farneth, W. (1978) *Chem. Rev. 78*, 125-145.
Valerie, K., Henderson, E. E., & DeRiel, J. K. (1985) *Proc. Natl. Acad. Sci. U.S.A. 82*, 4763-4767.
Van Camp, J. R., Young, T., Hartman, R. F., & Rose, S. D. (1987) *Photochem. Photobiol. 45*, 365-370.
Wurtman, R. J. (1975) *Sci. Am. 233*, 68-77.

Identification of Residues in the Insulin Molecule Important for Binding to Insulin-Degrading Enzyme†

Joseph A. Affholter,‡ Margaret A. Cascieri,§ Marvin L. Bayne,‖ Jens Brange,⊥ Monika Casaretto,# and Richard A. Roth*,‡

Department of Pharmacology, Stanford University School of Medicine, Stanford, California 94305, Departments of Biochemical Endocrinology and Growth Factor Research, Merck Sharp & Dohme Research Laboratories, Rahway, New Jersey 07065, Novo Research Institute, Novo Alle, DK-2880 Bagsvaerd, Denmark, and Deutsches Wollforschungsinstitut an der Technischen Hochschule Aachen, D-51 Aachen, Federal Republic of Germany

Received March 3, 1990; Revised Manuscript Received May 7, 1990

ABSTRACT: Insulin-degrading enzyme (IDE) hydrolyzes insulin at a limited number of sites. Although the positions of these cleavages are known, the residues of insulin important in its binding to IDE have not been defined. To this end, we have studied the binding of a variety of insulin analogues to the protease in a solid-phase binding assay using immunoimmobilized IDE. Since IDE binds insulin with 600-fold greater affinity than it does insulin-like growth factor I (25 nM and ~16 000 nM, respectively), the first set of analogues studied were hybrid molecules of insulin and IGF I. IGF I mutants [ins^{B1-17},17-70]IGF I, [Tyr^{55},Gln^{56}]IGF I, and [Phe^{23},Phe^{24},Tyr^{25}]IGF I have been synthesized and share the property of having insulin-like amino acids at positions corresponding to primary sites of cleavage of insulin by IDE. Whereas the first two exhibit affinities for IDE similar to that of wild type IGF I, the [Phe^{23},Phe^{24},Tyr^{25}]IGF I analogue has a 32-fold greater affinity for the immobilized enzyme. Replacement of Phe-23 by Ser eliminates this increase. Removal of the eight amino acid D-chain region of IGF I (which has been predicted to interfere with binding to the 23-25 region) results in a 25-fold increase in affinity for IDE, confirming the importance of residues 23-25 in the high-affinity recognition of IDE. A similar role for the corresponding (B24-26) residues of insulin is supported by the use of site-directed mutant and semisynthetic insulin analogues. Insulin mutants [B25-Asp]insulin and [B25-His]insulin display 16- and 20-fold decreases in IDE affinity versus wild-type insulin. Similar decreases in affinity are observed with the C-terminal truncation mutants [B1-24-His^{25}-NH_2]insulin and [B1-24-Leu^{25}-NH_2]insulin, but not [B1-24-Trp^{25}-NH_2]insulin and [B1-24-Tyr^{25}-NH_2]insulin. The truncated analogue with the lowest affinity for IDE ([B1-24-His^{25}-NH_2]insulin) has one of the highest affinities for the insulin receptor. Therefore, we have identified a region of the insulin molecule responsible for its high-affinity interaction with IDE. Although the same region has been implicated in the binding of insulin to its receptor, our data suggest that the structural determinants required for binding to receptor and IDE differ.

Insulin, insulin-like growth factor (IGF)[1] I, and insulin-like growth factor II constitute a family of hormones having a high degree of sequence and functional homology (Rinderknecht & Humbel, 1978a,b). Both insulin and IGF I have a number of growth-promoting effects, with the latter being identical with the growth-hormone-dependent somatomedin C (Klapper et al., 1983). A number of proteins have been described that are capable of binding with high affinity each member of the insulin/insulin-like growth factor (IGF) family. A unique cell-surface receptor exists for each of the peptides, which exhibits higher affinity for its specific ligand than for other membranes of the family [i.e., insulin receptor has the following order of affinities: insulin > IGF II > IGF I; for review, see Roth et al. (1988) and Czech (1989)]. In addition, serum binding proteins have been described that bind IGF I and IGF II but not insulin (Baxter & Martin, 1989). We have recently reported the molecular cloning and sequence analysis of another protein with differential affinities for insulin and the IGFs (Affholter et al., 1988). This protein—insulin-degrading enzyme (IDE)—is a cytosolic protease with a calculated molecular weight of 117 000 that shares structural and functional homology with bacterial protease III. In addition to hydrolyzing insulin in vitro, IDE appears to be re-

† This work was supported by NIH Grant DK34926 and an Advanced Predoctoral Fellowship awarded to J.A. by the Pharmaceutical Manufacturer's Association.
* Author to whom correspondence should be addressed.
‡ Stanford University School of Medicine.
‖ Department of Biochemical Endocrinology, Merck Sharp & Dohme Research Laboratories.
‖ Department of Growth Factor Research, Merck Sharp & Dohme Research Laboratories.
⊥ Novo Research Institute.
Deutsches Wollforschungsinstitut an der Technischen Hochschule Aachen.

[1] Abbreviations: IDE, insulin-degrading enzyme; IGF, insulin-like growth factor; EDTA, disodium ethylenediaminetetraacetate; PMSF, phenylmethanesulfonyl fluoride; BSA, bovine serum albumin.

0006-2960/90/0429-7727$02.50/0